

# Cyclic tests on RC joints retrofitted with pre-stressed steel strips and bonded steel plates

Yunlong Yu<sup>1,2</sup>, Yong Yang<sup>1,2</sup>, Yicong Xue<sup>\*1</sup>, Niannian Wang<sup>3</sup> and Yaping Liu<sup>4</sup>

<sup>1</sup>School of Civil Engineering, Xi'an University of Architecture & Technology, Shaanxi, China

<sup>2</sup>Key Lab of Structural Engineering and Earthquake Resistance, Ministry of Education, China

<sup>3</sup>Sichuan Provincial Architectural Design and Research Institute Co., LTD, SADI, Sichuan, China

<sup>4</sup>China Qiyuan Engineering Corporation, Shaanxi, China

(Received February 15, 2020, Revised April 3, 2020, Accepted April 13, 2020)

**Abstract.** An innovative retrofit method using pre-stressed steel strips and externally-bonded steel plates was presented in this paper. With the aim of exploring the seismic performance of the retrofitted RC interior joints, four 1/2-scale retrofitted joint specimens together with one control specimen were designed and subjected to constant axial compression and cyclic loading, with the main test parameters being the volume of steel strips and the existence of externally-bonded steel plates. The damage mechanism, force-displacement hysteretic response, force-displacement envelop curve, energy dissipation and displacement ductility ratio were analyzed to investigate the cyclic behavior of the retrofitted joints. The test results indicated that all the test specimens suffered a typical shear failure at the joint core, and the application of externally-bonded steel plates and that of pre-stressed steel strips could effectively increase the lateral capacity and deformability of the deficient RC interior joints, respectively. The best cyclic behavior could be found in the deficient RC interior joint retrofitted using both externally-bonded steel plates and pre-stressed steel strips due to the increased lateral capacity, displacement ductility and energy dissipation. Finally, based on the test results and the softened strut and tie model, a theoretical model for determining the shear capacity of the retrofitted specimens was proposed and validated.

**Keywords:** beam-column joints; pre-stressed steel strip; externally-bonded steel plate; retrofitting; pseudostatic test; shear capacity

## 1. Introduction

Non-seismically designed RC structures have suffered severe damage under moderate to severe earthquakes, and beam-column joints of these obsolete RC structures are generally subjected to large shear actions, which might suffer a brittle shear failure and even lead to the collapse of the entire building. Meanwhile, due to the lack of advanced seismic codes, most of the RC structures aforementioned were designed and built in late 1960s and early 1970s, when low-quality concrete and plain rebar without sufficient anchorage were generally applied and the amount of transverse reinforcements, namely stirrups, in structural components cannot meet the requirement of current seismic codes (Sezen *et al.* 2003, Engindeniz *et al.* 2005, Li *et al.* 2008, Rizwan *et al.* 2018, Rizwan *et al.* 2019, Ahmad *et al.* 2019a). Therefore, it has become a challenge to retrofit these obsolete RC structures to reduce the structural risk under the attack of earthquakes.

Many researchers have proposed the benefit of applying advanced materials in civil engineering, such as fiber reinforced polymer (FRP), to retrofit deficient RC structures (Ilki *et al.* 2011, Realfonzo *et al.* 2014, Singh *et al.* 2014, Kankeri *et al.* 2018, Marthong 2019, Barakat *et al.* 2019,

Antar *et al.* 2019). The application of FRP laminates or wraps is superior in durability and strength, but the cost of FRP products is currently much higher than that of steel products, which may be unaffordable for some builders. Therefore, the application of steel products, such as steel jacket, steel haunch and steel plate, in retrofitting is still the first choice of structural designers in the RC structures which do not need to suffer a harsh environment (Shafaei *et al.* 2014, Adibi *et al.* 2017, Akbar *et al.* 2018, Ahmad and Masoudi 2020). Among them, steel jacket cannot be applied in the retrofitting of interior RC joints due to the existence of transverse beams. For the retrofitting using steel haunch, although the steel haunch can confine the column and beam bottoms, the shear capacity of the joint core with inadequate stirrups cannot get enough enhancement to avoid the brittle shear failure. Nevertheless, steel haunches reduce shear demand on joint panels, therefore it has performed well under seismic loads, as confirmed by experimental and numerical studies (Ahmad *et al.* 2019b).

In order to solve the problems mentioned before, this paper presents an innovative retrofit method using pre-stressed steel strips and externally-bonded steel plates. The retrofitting using pre-stressed steel strips is a feasible strengthen method which can provide lateral confinement to structural components to enhance the concrete strength and lateral resistance (Helal 2012, Zhang *et al.* 2015, Yang *et al.* 2019). As shown in Fig. 1, some high-strength steel strips are assembled through the drilled tunnels in the transverse

\*Corresponding author, Ph.D., Associate Professor  
E-mail: [xjdxyc@foxmail.com](mailto:xjdxyc@foxmail.com)

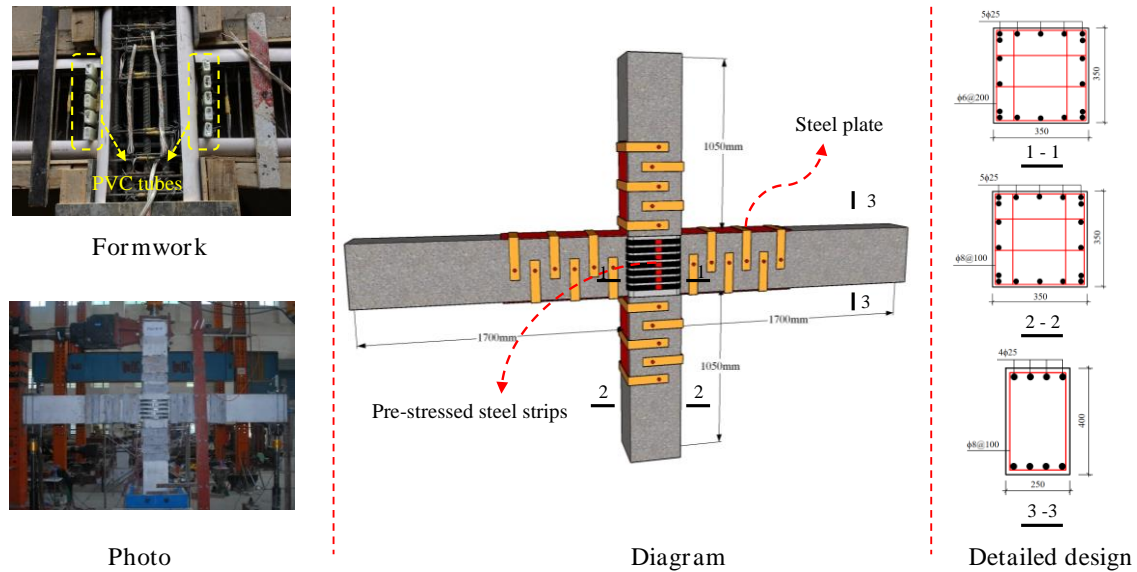


Fig. 1 Diagram of test specimens

Table 1 Specimens details

Specimen ID	Beam section (mm)	Column section (mm)	$\rho_s$ (%)	$n$	Retrofit	Spacing (mm)	Layers
J-1	250×400	350×350	0.36	0.2	-	-	-
J-2	250×400	350×350	0.36	0.2	Steel plates	-	-
SSJ-1	250×400	350×350	0.36	0.2	Steel strips+ Steel plates	50	3
SSJ-2	250×400	350×350	0.36	0.2	Steel strips+ Steel plates	50	3 (Gaps filled resin)
SSJ-3	250×400	350×350	0.36	0.2	Steel strips+ Steel plates	50	1

Note:  $n$  is the axial compression ratio, and  $\rho_s$  is the volumetric transverse reinforcement ratio at the joint core.

Table 2 Material properties

Material	Type	Diameter (mm)	Thickness (mm)	Width (mm)	$E_s$ (MPa)	$f_y$ (MPa)	$f_u$ (MPa)
Steel plate	Q235	-	8.0	250.0	$2.05 \times 10^5$	285.0	401.1
Steel strip	ULT980	-	0.9	31.8	$1.90 \times 10^5$	770.7	862.3
	HPB300	25	-	-	$2.00 \times 10^5$	435.2	607.5
Steel rebar	HRB400	8	-	-	$2.00 \times 10^5$	430.1	676.7
	HRB400	6	-	-	$2.00 \times 10^5$	389.2	578.3

beams, therefore, the joint core can be effectively confined and the shear capacity can be directly enhanced. Meanwhile, according to the softened strut and tie model (Hwang and Lee 2002), externally-bonded steel plates can be mounted on the top and bottom surfaces of the transverse beam and column to improve the flexural capacity, which can reinforce the major strut at the joint core to further enhance the shear capacity. Additionally, the proposed technique has less effect on altering the architecture of the structure, and it less affects the available space.

With the aim of exploring the seismic performance of the retrofitted RC interior joints, four 1/2-scale retrofitted joint specimens together with one control specimen were designed and subjected to constant axial compression and cyclic loading, with the main test parameters being the volume of steel strips and the existence of externally-bonded steel plates. The damage mechanism, force-

displacement hysteretic response, force-displacement envelop curve, energy dissipation and displacement ductility ratio were analyzed to investigate the cyclic behavior of the retrofitted joints. Based on the test results and the softened strut and tie model, a theoretical model for determining the shear capacity of the retrofitted specimens was proposed later in this paper.

## 2. Experimental program

### 2.1 Description of test specimens

As shown in Fig. 1, four 1/2-scale retrofitted joint specimens together with one control specimen were designed and subjected to constant axial compression and cyclic loading, and the main test parameters were the volume of steel strips and the existence of externally-

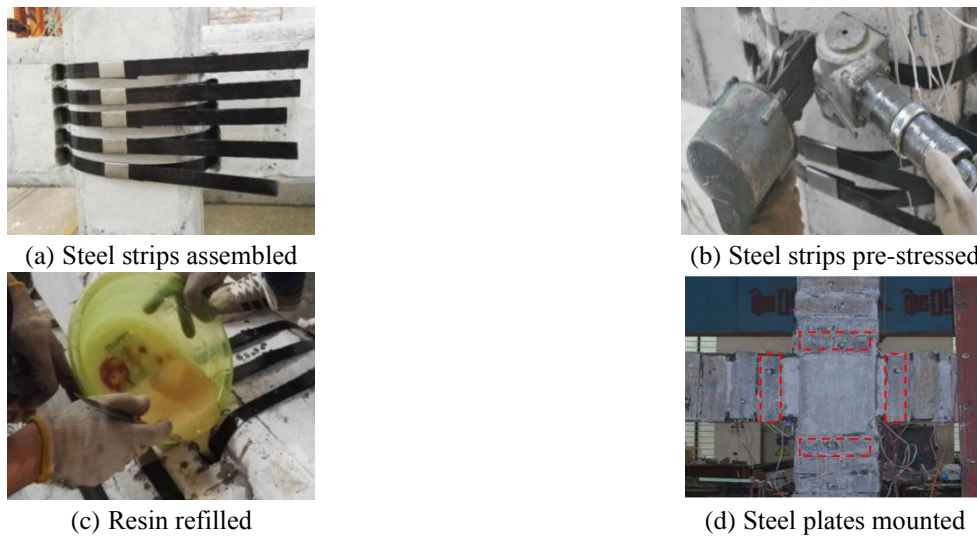


Fig. 2 Retrofit procedure

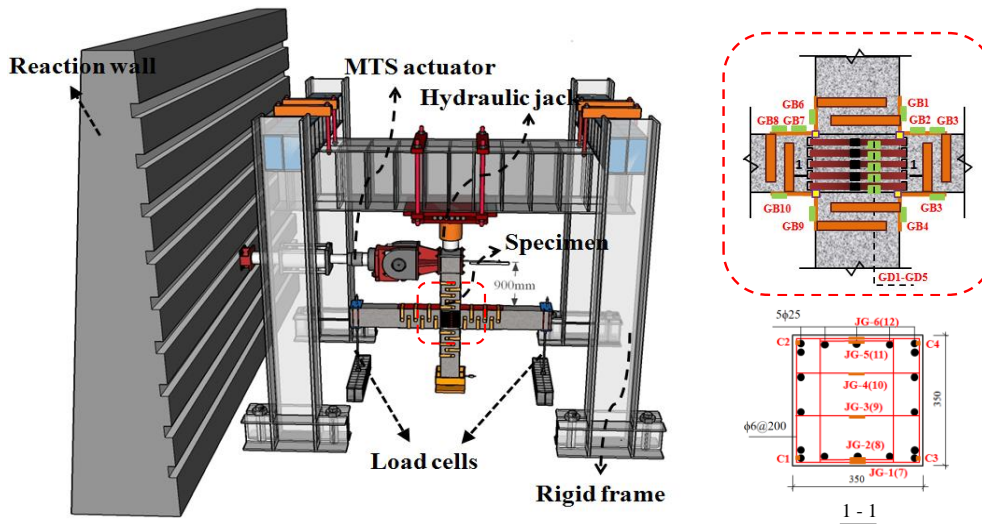


Fig. 3 Loading device and gauge arrangement

bonded steel plates. The height and width of the cross section were both 350 mm in the column and were 400 mm and 250 mm in the transverse beam. Meanwhile, the total height of the column was 2500 mm and the total length of the transverse beam was 3750 mm.

For the longitudinal reinforcements, the column of the specimens was reinforced using 18φ25 bars, indicating that the diameter of the rebar was 25 mm and the strength grade was HRB400 per Chinese codes, and the transverse beam of the specimens was reinforced by 8φ25 bars. For the transverse reinforcements, both the stirrups in the transverse beam and column were φ8 bars with a spacing of 200 mm. The joint core area was transversely reinforced by the rebar with a diameter of 6 mm and the grade of HPB300, and the spacing of the adjacent ribs was 200 mm to simulate the deficient RC joints with inadequate stirrups.

The axial compression ratio of the joint specimens in the test was both 0.2, indicating that the corresponding design axial compression ratio of these joints was approximately 0.4, which was common in the seismically-designed RC

structures in China. Other details of the test specimens are listed in Table 1.

## 2.2 Material properties

The concrete strength was designed as C30 grade to simulate the concrete in decades-old RC structures. Normal-weight and ready-mixed concrete was applied in all the specimens, and some standard concrete cubes with the dimensions of 150 mm×150 mm×150 mm were prepared together with the specimens casting and were cured with the same condition as the joint specimens. The compression test on these concrete cubes was conducted when the joint specimens were tested, and the average 28-day cubic compressive strength was 25.4 MPa.

The width and thickness of the high-strength steel strips were 31.8 mm and 0.9 mm, respectively, and the average measured yield strength and ultimate strength of the strip coupons were 770.71 MPa and 862.33 MPa, respectively. The detailed mechanical properties of the rebar and the steel plates are listed in Table 2.

### 2.3 Retrofit procedure

The retrofit procedure can be divided into four individual steps.

In the first step, as shown in Fig. 2(a), the steel strips were bent into hoops and assembled at the target location. In this test, some tunnels were prefabricated in the transverse beam using PVC tubes before the concrete was cast, and in practical applications, these tunnels in the beam web can be drilled using drilling machine. Because the longitudinal reinforcements in the transverse beam were usually located near the top and bottom surfaces, the damage caused by the drilled tunnels near the beam web, which would be refilled using high-strength grout later, usually could only cause a slight strength reduction.

In the second step, as shown in Fig. 2(b), a stretching tool powered by air pump was applied to pre-stress these placed steel strips. During the retrofit process, some strain gauges were mounted on the strips to monitor the tensile strain, and the results indicated that average tensile stress was approximately 80 MPa, which is 10% of the tensile yield strength of the applied steel strip. After that, some notches for locking the strip connectors to maintain the tensile force were made using a pneumatic fastening jaw.

In the third step, as shown in Fig. 2(c), the drilled tunnels in the transverse beam were refilled using resin. Because some gaps would appear between the different layers of the steel strips, in this step, the gaps between the different strip layers in one of the test specimens were filled using resin to explore the retrofit efficiency of the specimens retrofitted using multiple-layer strips.

In the last step, as shown in Fig. 2(d), some steel plates were fixed on the top and bottom surfaces of the column and the transverse beam using structural glue and U-shaped hoops. In practical applications, epoxy mortar should be used for attaching steel plates and strips to enhance the durability.

### 2.4 Test procedure

The test device and the layout of the applied strain gauges are illustrated in Fig. 3. As shown in Fig. 3, during the test process, the column bottom was restrained by a steel hinge which was mounted on the strong floor, and the two beam ends of the joint specimens were supported using steel rollers to restrain their vertical displacements and to allow the horizontal displacements and rotations. A constant compressive load was vertically applied on the column top by a 1000 kN hydraulic jack, and then the reversed lateral load was applied at the column top through a 1000 kN actuator.

During the test, the deformations of the transverse beam, column and the joint distortion were monitored using six linear variable displacement transducers (LVDTs), among which the joint distortion was measured by two cable LVDTs. The vertical load applied on the column top was monitored by a pressure gauge affiliated to the oil jack, and the corresponding lateral load was recorded by the loading system. Meanwhile, the reactions at the beam ends could be measured using two load cells which were attached to the steel rollers.

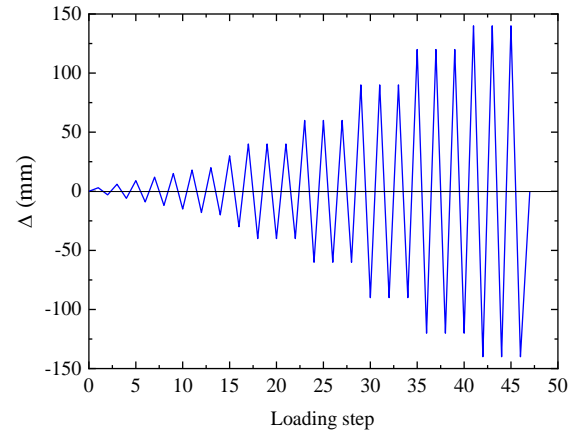


Fig. 4 Loading protocol

As shown in Fig. 4, the lateral load was controlled using a displacement-controlled loading protocol during the test, and the distance from the lateral loading point to the bottom support was 2350 mm. Before the longitudinal reinforcements of the specimens yielded, the amplitude of horizontal displacement was increased by 3 mm each cycle. After that, the amplitude of horizontal displacement was increased by 20 mm with each cycle repeated three times at the same drift ratio. When the horizontal load fell by more than 20% of the experienced peak load or the horizontal displacement of the column top was over the maximum displacement of the oil jack (120 mm), the test terminated.

## 3. Experimental results

### 3.1 Damage mechanism

The crack patterns of the specimens are shown in Fig. 5, where the photos in the first column, second column and third column show the crack patterns when the specimens reached the corresponding yield load, peak load and ultimate load, respectively.

Fig. 5(a) shows the crack propagation progress of the control specimen J-1 without any retrofitting. At the beginning of the test, the vertical cracks were initially found in the transverse beam, and then the first inclined crack could be observed at the joint core. With the load increasing, the vertical cracks in the transverse beam propagated slowly and the inclined cracks at the joint core developed into X-shaped cross crack bands rapidly due to load reversal. When the drift ratio was approximately 2.4%, the major inclined crack at the joint core widened suddenly, which led to the yielding of the stirrups. When the test terminated, an apparent spalling of concrete cover at the joint core could be observed, indicating that the control specimen suffered a typical shear failure at the joint core.

Fig. 5(b) shows the crack propagation progress of the specimen J-2 retrofitted only using externally-bonded steel plates. The overall crack pattern of this specimen was similar to that of the specimen J-1, but the much severer spalling of concrete was observed in the specimen J-2. The main reason might be that the increased longitudinal

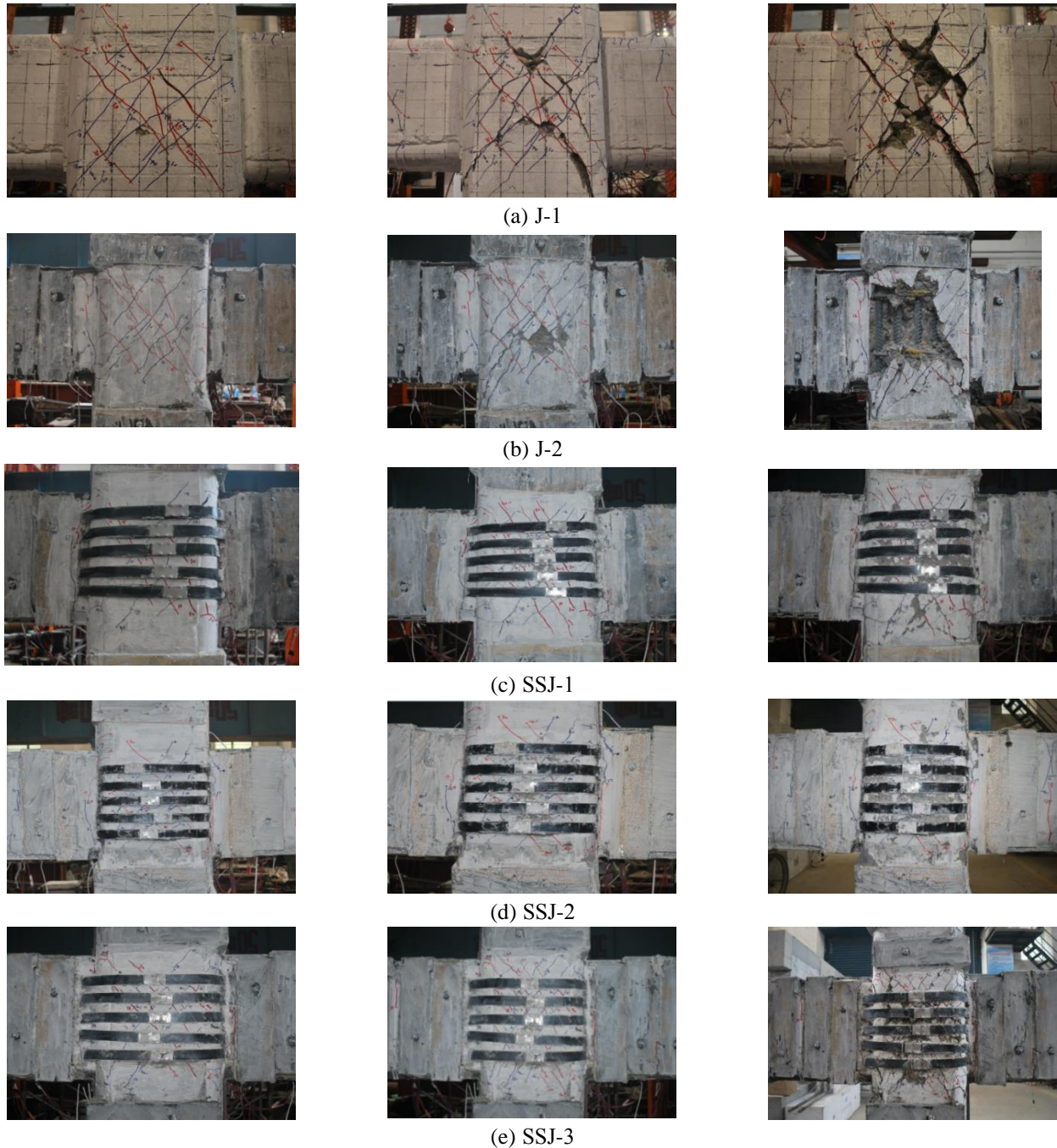


Fig. 5 Crack pattern and damage mechanism

reinforcements applied in the transverse beam and column led to a larger height of the major compressive strut formed at the joint core, which could induce more shear action and cause additional damage in this area.

Fig. 5(c) to Fig. (e) show the crack propagation progresses of the specimens retrofitted using pre-stressed strips together with externally-bonded steel plates. Generally, the crack development of these specimens was similar to that of the specimens J-1 and J-2 at the beginning of the test. Instead of severe spalling of core concrete, when the drift ratio was approximately 4.8%, the concrete at the joint core, which was strengthened using pre-stressed steel strips, spalled from the gaps between the steel strips. When

the test terminated, only slight dilation of cover concrete could be found at the joint core, indicating that the core concrete was effectively confined to avoid spalling. Meanwhile, attributed to the application of steel strips, abundant cracks were captured at the joint core, indicating that only a slight damage was shown in these retrofitted specimens as compared with the severe concrete spalling of the specimens J-1 and J-2.

### 3.2 Force-displacement hysteretic response and force-displacement envelop curve

Fig. 6 depicts the force-displacement hysteretic

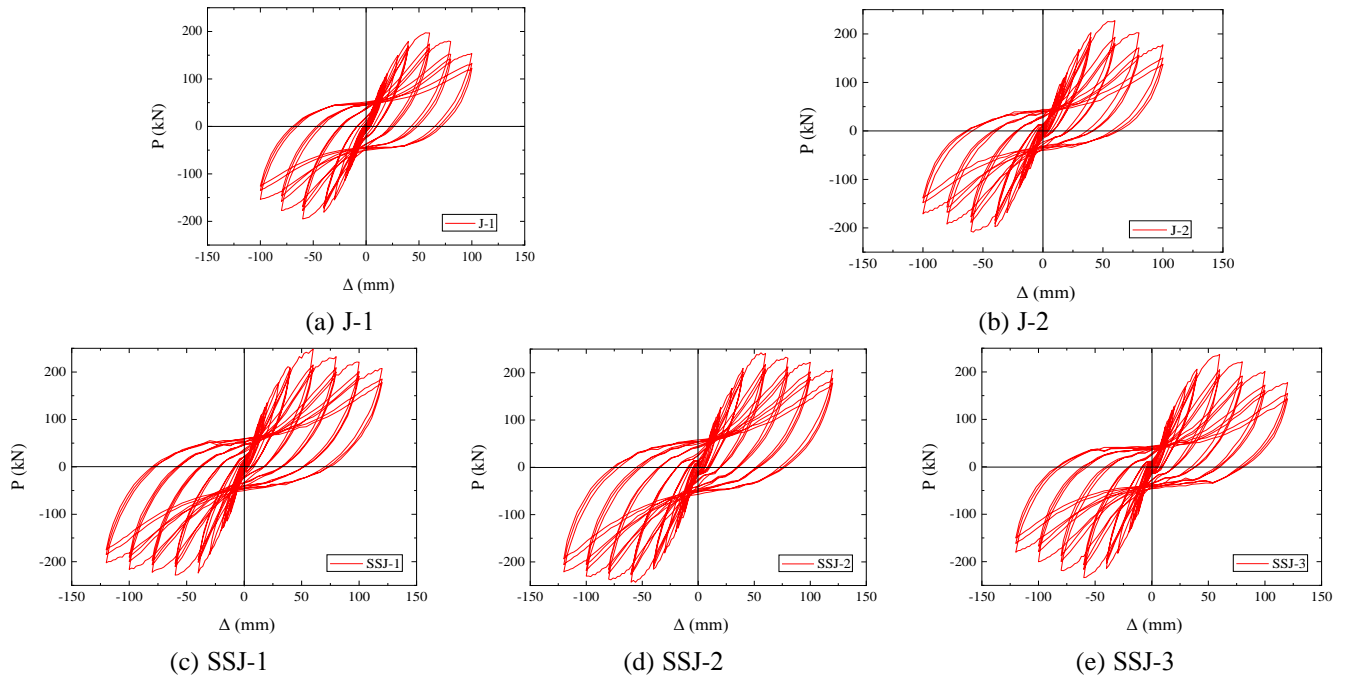


Fig. 6 Force-displacement hysteretic response

Table 3 Test results

ID	Loading direction	$\Delta_y$ (mm)	$P_y$ (kN)	Average $P_y$	$P_m$ (kN)	Average $P_m$	$\Delta_u$ (mm)	Average $\Delta_u$	$\mu$	Average $\mu$
J-1	Push	39.12	177.86	177.20	196.86	195.89	89.60	89.77	2.29	2.24
	Pull	41.07	176.54		194.92		89.94		2.19	
J-2	Push	42.26	208.41	199.75	227.37	217.16	86.60	91.15	2.05	2.33
	Pull	36.86	191.09		206.94		95.70		2.60	
SSJ-1	Push	43.55	218.70	213.70	248.10	238.25	115.39	120.25	2.65	3.11
	Pull	35.19	208.69		228.39		125.10		3.56	
SSJ-2	Push	40.88	212.22	218.93	242.83	241.84	127.23	123.97	3.11	2.91
	Pull	44.54	225.63		240.85		120.71		2.71	
SSJ-3	Push	43.38	214.14	212.12	236.82	235.30	99.93	100.74	2.30	2.48
	Pull	38.25	210.10		233.77		101.55		2.66	

responses of the test specimens, and Table 3 lists the main results of the specimens. As shown in Fig. 6, in all the specimens, the load-displacement relationship remained elastic at the beginning of the test, and the area of the single loop increased after the specimens yielded. At the failure stage, all the specimens suffered a pinched hysteretic behavior, indicating the slippage between rebar and concrete occurred during the re-loading period. Nevertheless, the specimen J-1 without any retrofitting exhibited the largest residual deformation among the test specimens, indicating that the good anchorage of the externally-bonded steel plates could reduce the pinching effect of the deficient RC joints and lead to a higher energy dissipation capacity. Meanwhile, the retrofitted specimens also exhibited robust force-displacement hysteretic responses than the control specimen, indicating that the application of pre-stressed steel strips and externally-bonded steel plates could enhance both the deformability and the lateral capacity.

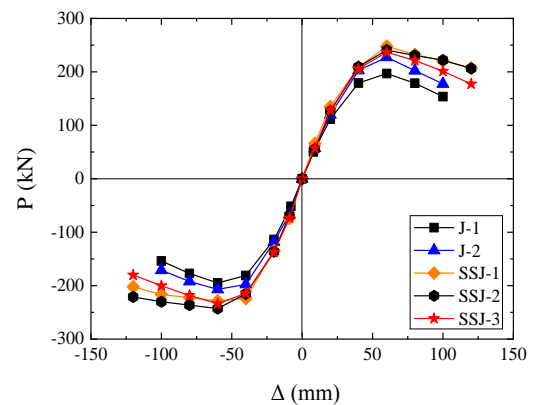


Fig. 7 Force-displacement envelop curve

Fig. 7 shows the comparison of force-displacement envelop curves of different specimens. As shown in Fig. 7 and Table 3, the lateral capacity and ultimate displacement of the

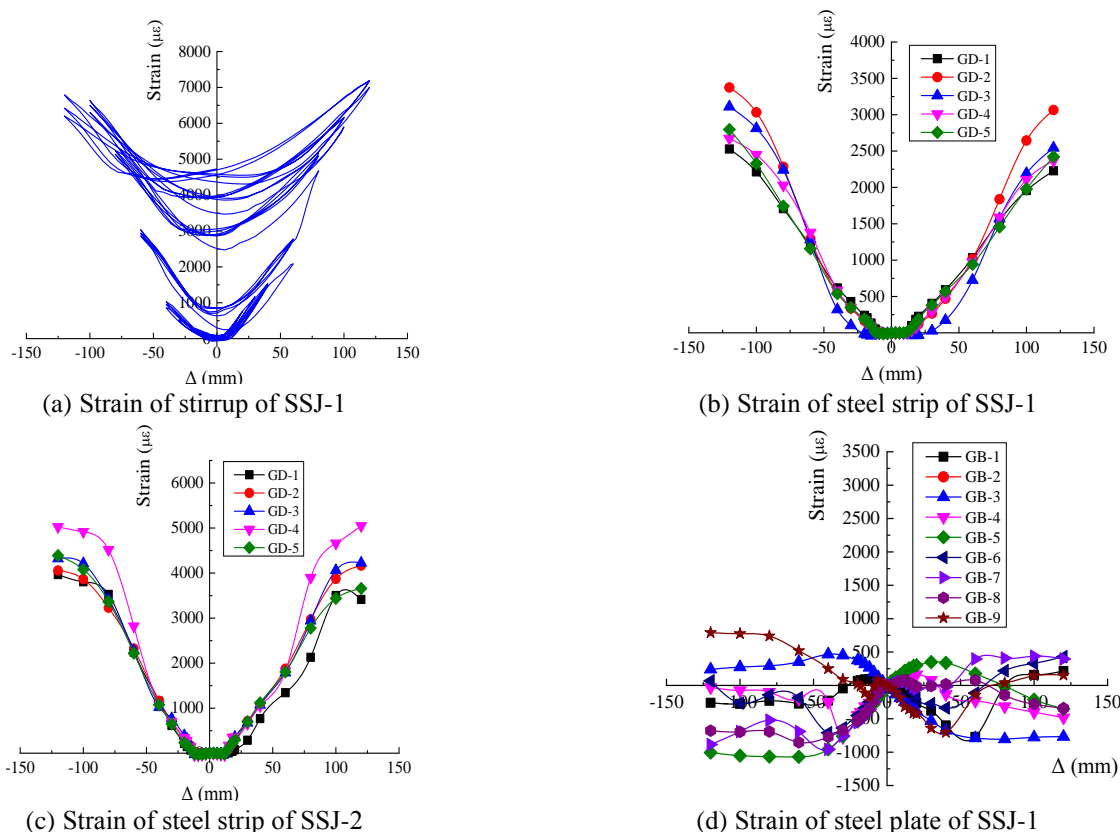


Fig. 8 Strain result

specimen J-2 were 1.11 and 1.02 times greater than those of the specimen J-1, and the lateral capacity and ultimate displacement of the specimen SSSJ-1 were 1.21 and 1.34 times greater than those of the specimen J-1. It indicated that the application of externally-bonded steel plates could only increase the lateral capacity of the deficient RC joint, but the application of pre-stressed steel strips could both increase the lateral capacity and the deformability. The main reason was that the application of steel plates reinforced the major compressive strut at the joint core, which could directly increase the lateral capacity, but deformability could be only enhanced by the lateral confinement provided by the steel strips. Meanwhile, the lateral capacities of the specimens SSSJ-1 and SSSJ-3 were comparative, but the ultimate displacement of the specimen SSSJ-1 was 1.19 times greater than that of the specimen SSSJ-3, indicating that the deformability of the retrofitted specimens was primarily related to the volume of steel strips. What is noticeable was that the increase of strip volume without the application of externally-bonded steel plates could only increase the deformability, indicating that the combination of pre-stressed steel strips and externally-bonded steel plates could bring an additional benefit.

### 3.3 Strain analysis

Fig. 8 shows the strain results of the test specimens.

As shown in Fig. 8(a), in the specimen SSSJ-1, the stirrups yielded before the corresponding peak load reached, and the stirrup strain when the test terminated was over 3

times greater than the yield strain. It indicated that the joint core was subjected to a large shear action and suffered a typical shear failure, which was consistent with the test observation mentioned before.

As shown in Fig. 8(b) and Fig. 8(c), the strain of the steel strips of the outermost layer in the specimen SSSJ-1 was lower than the corresponding yield strain, but that in the specimen SSSJ-2, in which the gaps between the different strip layers were filled using resin, reached the yield strain. It indicated that the gaps between the different strip layers led to a loss in stress transfer when the joint core was confined, which would also result in a low retrofit efficiency when multiple-layer strips were applied. Therefore, in practical applications, larger pre-stress should be applied in the steel strips to eliminate these gaps.

As shown in Fig. 8(d), the externally-bonded steel plates almost reached the corresponding yield strain, indicating that these steel plates did play an important role in the shear behavior of the retrofitted specimens through increasing the height of the compression zone at the beam and column bottoms, which could lead to an increase of the total height of the major compressive strut at the joint core.

### 3.4 Ductility

The ductility ratio can be calculated using the ultimate displacement  $\Delta_u$  dividing the yielding displacement  $\Delta_y$  at the lateral loading point. The ultimate displacement  $\Delta_u$  was determined as the lateral displacement of the joint when the lateral load fell by more than 20% of the experienced peak

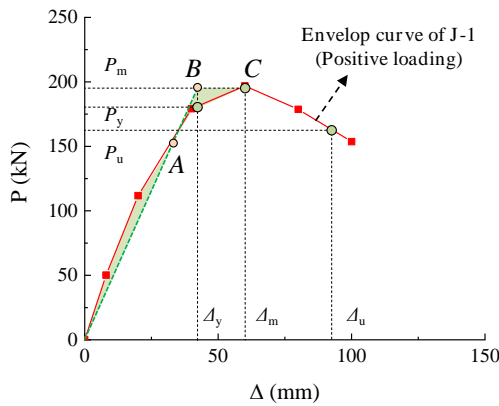


Fig. 9 Calculation of ductility ratio

load, and the yielding displacement  $\Delta_y$  was obtained using a graphic method. As shown in Fig. 9, a secant  $OB$  which passes the zero point is drawn to intersect the force-displacement envelop curve at point  $A$  to ensure that the area enclosed by points  $A$ ,  $B$  and  $C$  is equal to the area enclosed by line  $OA$  and the force-displacement envelop curve. The vertical projection of point  $B$  on the force-displacement envelop curve can be regarded as the yield point.

The calculated ductility ratios of the test specimens were recorded in Table 3. As shown in Table 3, the specimen J-2 exhibited the comparative displacement ductility with the specimen J-1, and the ductility ratio of the specimen SSJ-1 was 1.39 times greater than that of the specimen J-1. It indicated that the application of externally-bonded steel plates cannot enhance the deformability of the deficient RC joints with inadequate core stirrups, whereas the combination of pre-stressed steel strips and externally-bonded steel plates can effectively improve both the lateral capacity and the ductility. Meanwhile, the ductility ratio of the specimen with a lower strip volume was lower than that of the specimen with a higher strip volume, indicating the ductility was highly related to the strip volume.

### 3.5 Energy dissipation

The area enclosed by the force-displacement hysteretic response can be regarded as the energy dissipated during each cycle of lateral loading, and the cumulative energy dissipation is the accumulation of the energy dissipated before the current circle. The cumulative energy dissipation of the test specimens when the test terminated can be found in Fig. 10. As shown in Fig. 10, the parameters which affected the energy dissipation almost followed the same trend as those which affected the ductility. The cumulative energy dissipation of the specimen SSJ-1 was 1.54 times greater than that of the control specimen J-1, which could be attributed to the enhancements both in the lateral capacity and the deformability. What is noticeable was that the energy dissipation of the specimen SSJ-1 and that of the specimen SSJ-2 were nearly the same, indicating that refilling the strip gaps was not necessary in practical applications. Meanwhile, as could be seen from the energy

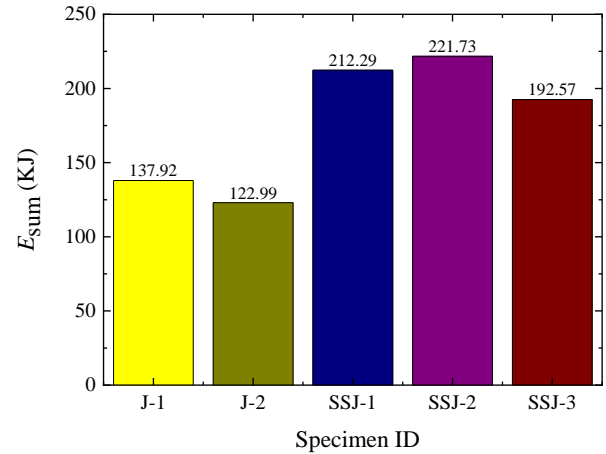


Fig. 10 Cumulative energy dissipation

dissipation of the specimen SSJ-1 and that of the specimen SSJ-3, the the energy dissipation of the retrofitted specimens increased with the increase of the strip volume.

To conclude, the application of pre-stressed steel strips and externally-bonded steel plates can enhance the lateral capacity, ductility and energy dissipation of deficient RC interior joints simultaneously. Meanwhile, it should be noticed that the reinforcement ratios of the transverse beam and column were designed higher than usual deliberately to investigate the shear capacity of the joint core in this research, but in the practical obsolete RC structures, the final failure might be migrated away from the joint core due

to the enhanced joint strength provided by the pre-stressed steel strips and externally-bonded steel plates.

## 4. Shear capacity

A simplified softened strut and tie model (SST) proposed by Hwang and Lee (2002) is modified here to calculate the shear capacity of the retrofitted specimens. As illustrated in Fig. 11, the SST model was established by the vertical, horizontal and diagonal mechanisms based on the equilibrium condition, compatible condition and constitutive laws.

The shear capacity of the RC beam-column joint can be obtained from the following equations:

$$V_j = K\zeta f_c A_{str} \cos \theta \quad (1)$$

$$\zeta = 0.79 - \frac{f_c}{200} \quad (2)$$

$$A_{str} = a_s \times b_s \quad (3)$$

$$a_s = \sqrt{c_b^2 + c_c^2} = \sqrt{\left(\frac{A_s f_y}{0.85 \beta_1 f_c b_b}\right)^2 + \left[(0.25 + 0.85 \frac{N}{f_c A_c}) h_c\right]^2} \quad (4)$$

where  $\zeta$  is the softened ratio of concrete proposed by Nielsen (1984);  $K$  is the SST index;  $A_{str}$  is the cross-sectional area of the major compressive strut at the joint core;  $f_c$  is the compressive strength of concrete;  $b_s$  and  $a_s$  are

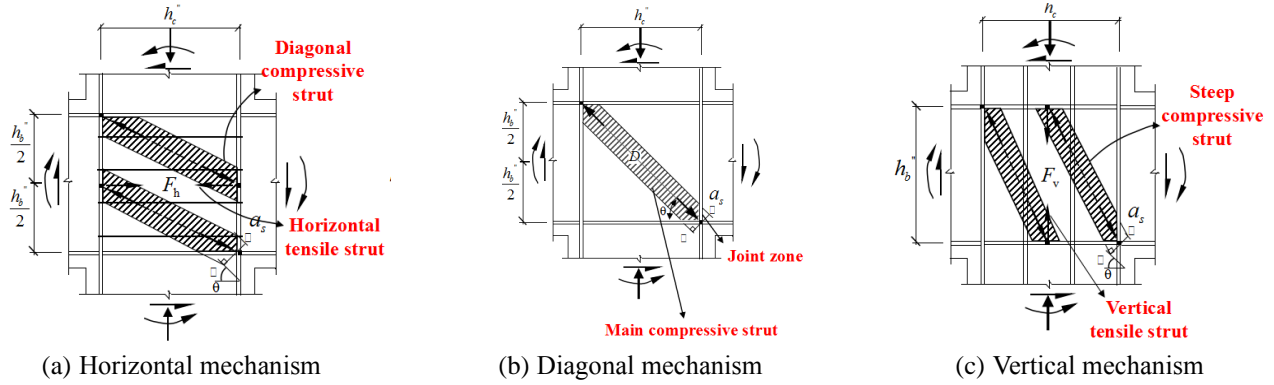


Fig. 11 shear-resisting mechanism at joint core

the cross-sectional width and height of the major compressive strut;  $\theta$  is the angle between the horizontal axis and the major compressive strut;  $c_c$  and  $c_b$  are the cross-sectional heights of the compressive zone of the column bottom and that of the beam bottom.

The SST index can be calculated as:

$$K = K_h + K_v - 1 \quad (5)$$

where  $K_h$  is the horizontal tie index;  $K_v$  is the vertical tie index.

The horizontal tie index can be calculated as:

$$\overline{K}_h \approx \frac{1}{1 - 0.2(\gamma_h + \gamma_h^2)} \quad (6)$$

$$K_h = 1 + \frac{(\overline{K}_h - 1)(A_{th}f_{yh} + A_{ss}f_{ys})}{F_h}, \quad K_h < \overline{K}_h \quad (7)$$

$$\gamma_h = \frac{2 \tan \theta - 1}{3} \quad (8)$$

where  $A_{th}$  and  $A_{ss}$  are the cross-sectional areas of the stirrup and the steel strip;  $f_{yh}$  and  $f_{ys}$  are the yield strengths of the stirrup and the steel strip. The meanings of other variables in Eqs. (6)-(8) are the same as the SST model proposed by Hwang and Lee (2002), and the vertical tie index,  $K_v$ , can be determined following a similar procedure.

For the retrofitted specimens, the cross-sectional heights of the compressive zone of the beam bottom and that of the column bottom are increased due to the application of externally-bonded steel plates. Therefore, Eq. (4) can be modified as:

$$c_b = \frac{A_s f_y + A_{sp} f_{yp}}{0.85 \beta_1 f_c b_b} \quad (9)$$

where  $A_{sp}$  and  $A_s$  are the cross-sectional areas of the steel plate and the longitudinal rebar;  $f_{yp}$  and  $f_y$  are the yield strengths of the steel plate and the longitudinal rebar;  $\beta_1$  is a ratio in the equivalent rectangle stress method;  $b_b$  is the cross-sectional width of the transverse beam.

The measured and calculated results are recorded in Table 4. The average value of the ratios of the calculated to

Table 4 Tested and calculated shear capacity

ID	Tested shear force in upper column $V_{uc}$ (kN)	Tested shear force in beam bottom $V_{bb}$ (kN)	Calculated shear capacity of joint zone $V_c$ (kN)	Tested shear capacity of joint zone $V_e$ (kN)	$V_c / V_e$
J -1	195.89	142.95	1064.28	1149.47	0.93
J -2	217.15	166.16	1413.82	1346.73	1.05
SSJ-1	238.24	178.12	1590.13	1438.21	1.11
SSJ-2	241.84	179.02	1590.13	1443.01	1.10
SSJ-3	235.29	177.95	1478.54	1439.51	1.03
Average value					1.04
Coefficient of variation					0.06

tested capacities is 0.93, and the coefficient of variation is 0.10, indicating that the proposed method can calculate the shear capacity of the retrofitted specimens reasonably.

## 5. Conclusions

This paper presents an experimental and theoretical research on the cyclic behavior of deficient RC interior joints retrofitted using pre-stressed steel strips and externally-bonded steel plates. A total of five 1/2-scale joint specimens were designed and subjected to axial compression and lateral loading, and the following conclusions can be drawn:

Both the control specimen and retrofitted specimens suffered typical shear failures at the joint core. The control specimen without any retrofitting exhibited severe concrete spalling at the joint core area. Nevertheless, attributed to the application of steel strips, abundant cracks were captured at the joint core of the retrofitted specimens, indicating that only a slight damage was shown in the retrofitted specimens as compared with the severe concrete spalling of the control specimen. Meanwhile, the application of externally-bonded steel plates could effectively decrease the damage occurred on the transverse beam.

The retrofitted specimens could exhibit higher lateral capacity, greater displacement ductility and higher energy dissipation as compared with the control specimen. Among the test specimens, the application of externally-bonded

steel plates could only enhance the lateral capacity, but the combination of pre-stressed steel strips and externally-bonded steel plates could effectively improve both the lateral capacity and the displacement ductility. Meanwhile, the deformability of the deficient RC joints with inadequate stirrups was highly related to the strip volume, and the energy dissipation and ductility of the retrofitted specimens increased with the increase of the strip volume.

The gaps between the different strip layers were inevitable in practical applications. Although these gaps could lead to a loss in stress transfer when multiple-layer strips were applied, the energy dissipation of the gap-refilled specimen and that of its control specimen were nearly the same, indicating that refilling the strip gaps was not necessary in practical applications.

Based on the test results, a simplified softened strut and tie model was proposed to calculate the shear capacity of the test specimens. The average value of the ratios of the calculated to tested capacities is 0.93, and the coefficient of variation is 0.10, indicating that the proposed method can calculate the shear capacity of the retrofitted specimens reasonably.

## Acknowledgements

The experiments were sponsored by the National Natural Science Foundation of China (Grant No.51908450 and No. 51978565). The financial support is highly appreciated.

## References

- Adibi, M., Marefat, M.S., Esmaily, A., Arani, K.K. and Esmaily, A. (2017), "Seismic retrofit of external concrete beam-column joints reinforced by plain bars using steel angles prestressed by cross ties", *Eng. Struct.*, **148**, 813-828. <https://doi.org/10.1016/j.engstruct.2017.07.014>.
- Ahmad, N., Shahzad, A., Rizwan, M., Khan, A.N., Ali, S.M., Ashraf, M., Naseer, A., Ali, Q. and Alam, B. (2019a), "Seismic performance assessment of non-compliant SMRF reinforced concrete frame: shake-table test study", *J. Earthq. Eng.*, **23**(3), 444-462. <https://doi.org/10.1080/13632469.2017.1326426>.
- Ahmad, N., Akbar, J., Rizwan, M., Alam, B., Khan, A.N. and Lateef, A. (2019b), "Haunch retrofitting technique for seismic upgrading deficient RC frames", *Bullet. Earthq. Eng.*, **17**(7), 3895-3932. <https://doi.org/10.1007/s10518-019-00638-9>.
- Ahmad, N. and Masoudi, M. (2020), "Eccentric steel brace retrofit for seismic upgrading of deficient reinforced concrete frames". *Bullet. Earthq. Eng.*, **18**(6), 2807-2841. <https://doi.org/10.1007/s10518-020-00808-0>.
- Akbar, J., Ahmad, N., Alam, B. and Ashraf, M. (2018), "Seismic performance of RC frames retrofitted with haunch technique", *Struct. Eng. Mech.*, **67**(1), 1-8. <https://doi.org/10.12989/sem.2018.67.1.001>.
- Antar, K., Amara, K., Benyoucef, S., Bouazza, M. and Ellali, M. (2019), "Hygrothermal effects on the behavior of reinforced-concrete beams strengthened by bonded composite laminate plates", *Struct. Eng. Mech.*, **69**(3), 327-334. <https://doi.org/10.12989/sem.2019.69.3.327>.
- Barakat, S., Al-Toubat, S., Leblouba, M. and Burai, E.A. (2019), "Behavioral trends of shear strengthened reinforced concrete beams with externally bonded fiber-reinforced polymer", *Struct. Eng. Mech.*, **69**(5), 579-589. <https://doi.org/10.12989/sem.2019.69.5.579>.
- Engindeniz, M., Kahn, L.F. and Abdul-Hamid, Z. (2005), "Repair and strengthening of reinforced concrete beam-column joints: State of the art", *ACI Struct. J.*, **102**(2), 187-197.
- Helal, Y. (2012), "Seismic strengthening of deficient exterior RC beam-column sub-assemblages using post-tensioned metal strips", Ph.D. Dissertation, University of Sheffield, Sheffield. <http://etheses.whiterose.ac.uk/id/eprint/7286>.
- Hwang, S.J. and Lee, H.J. (2002), "Strength prediction for discontinuity regions by softened strut-and-tie model", *J. Struct. Eng.*, **128**(12), 1519-1526. [https://doi.org/10.1061/\(ASCE\)0733-9445\(2002\)128:12\(1519\)](https://doi.org/10.1061/(ASCE)0733-9445(2002)128:12(1519)).
- Ilki, A., Bedirhanoglu, I. and Kumbasar, N. (2011), "Behavior of FRP-retrofitted joints built with plain bars and low-strength concrete", *J. Compos. Construct.*, **15**(3), 312-326. [https://doi.org/10.1061/\(ASCE\)CC.1943-5614.0000156](https://doi.org/10.1061/(ASCE)CC.1943-5614.0000156).
- Kankeri, P., Prakash, S.S. and Pachalla, S.K.S. (2018), "Analytical and numerical studies on hollow core slabs strengthened with hybrid FRP and overlay techniques", *Struct. Eng. Mech.*, **65**(5), 535-546. <https://doi.org/10.12989/sem.2018.65.5.000>.
- Li, H., Xiao, S. and Huo, L. (2008), "Damage investigation and analysis of engineering structures in the Wenchuan earthquake", *J. Build. Struct.*, **29**(4), 10-19. (in Chinese)
- Marthong, C. (2019), "Rehabilitation and strengthening of exterior RC beam column connections using epoxy resin injection and FRP sheet wrapping: Experimental study", *Struct. Eng. Mech.*, **72**(6), 723-736. <https://doi.org/10.12989/sem.2019.72.6.723>.
- Nielsen, M.P. (1984), *Limit Analysis and Concrete Plasticity*, Prentice-Hall, Upper Saddle River, New Jersey, USA.
- Realfonzo, R., Napoli, A. and Pinilla, J.G.R. (2014), "Cyclic behavior of RC beam-column joints strengthened with FRP systems", *Construct. Build. Mater.*, **54**, 282-297. <https://doi.org/10.1016/j.conbuildmat.2013.12.043>.
- Rizwan, M., Ahmad, N. and Khan, A.N. (2019), "Seismic performance of RC frame having low strength concrete: experimental and numerical studies", *Earthq. Struct.*, **17**(1), 75-89. <https://doi.org/10.12989/eas.2019.17.1.075>.
- Rizwan, M., Ahmad, N. and Khan, A. N. (2018), "Seismic performance of compliant and noncompliant special moment-resisting reinforced concrete frames", *ACI Struct. J.*, **115**(4), 1063-1073.
- Sezen, H., Whittaker, A.S., Elwood, K.J. and Mosalam, K.M. (2003), "Performance of reinforced concrete buildings during the August 17, 1999 Kocaeli, Turkey earthquake, and seismic design and construction practise in Turkey", *Eng. Struct.*, **25**(1), 103-114. [https://doi.org/10.1016/S0141-0296\(02\)00121-9](https://doi.org/10.1016/S0141-0296(02)00121-9).
- Shafaei, J., Hosseini, A. and Marefat, M.S. (2014), "Seismic retrofit of external RC beam-column joints by joint enlargement using prestressed steel angles", *Eng. Struct.*, **81**, 265-288. <https://doi.org/10.1016/j.engstruct.2014.10.006>.
- Singh, V., Bansal, P.P., Kumar, M. and Kaushik, S.K. (2014), "Experimental studies on strength and ductility of CFRP jacketed reinforced concrete beam-column joints", *Construct. Build. Mater.*, **55**, 194-201. <https://doi.org/10.1016/j.conbuildmat.2014.01.047>.
- Yang, Y., Xue, Y., Yu, Y. and Li, Y. (2019), "Research on axial behaviour of concrete columns retrofitted with pre-stressed steel strips", *Mag. Concrete Res.*, 1-13. (Online first). <https://doi.org/10.1680/jmacr.18.00107>.
- Zhang, B., Yang, Y., Wei, Y.F., Liu, R.Y., Ding, C. and Zhang, K.Q. (2015), "Experimental study on seismic behavior of reinforced concrete column retrofitted with prestressed steel strips", *Struct. Eng. Mech.*, **55**(6), 1139-1155. <https://doi.org/10.12989/sem.2015.55.6.1139>.